DOI:
10.1038/s41598-019-53565-9

Dear Editor of Neuroimage,

On behalf of all authors, I would like to submit the manuscript “Tensor Decomposition of TMS-induced EEG oscillations reveals data-driven profiles of antiepileptic drug effects”. In this work, we reveal the effects of antiepileptic drugs on the TMS-induced EEG data using the data-driven approach (a so called tensor decomposition technique). This work is original, has it has never been submitted or under review in any journal.

Best regards,

Chayanin Tangwiriyasakul (PhD)

Tensor decomposition of TMS-induced EEG oscillations reveals data-driven profiles of antiepileptic drug effects

C. Tangwiriyasakul[1]*, I. Premoli[1]*, L. Spyrou[2], R.F. Chin[3], J. Escudero[2**], and M.P. Richardson[1**]

[1] Department of Basic and Clinical Neuroscience, Institute of Psychiatry, Psychology and Neuroscience (IoPPN), King's College London, London, UK.

[2] School of Engineering, Institute for Digital Communications, The University of Edinburgh, Thomas Bayes Rd, Edinburgh EH9 3FG, UK

[3] Muir Maxwell Epilepsy Centre, Centre for Clinical Brain Sciences, The University of Edinburgh, West Mains Rd, Edinburgh EH9 3FB, UK

*These authors share first authorship

**These authors share senior authorship

Corresponding author: Chayanin Tangwiriyasakul, King's College London, Insitute of Psychiatry Psychology and Neuroscience, London, UK. Email: chayanin.tangwiriyasakul@kcl.ac.uk

Running title: Tensor Decomposition in TMS-EEG

Keywords: TMS-EEG, antiepileptic drugs, tensor decomposition, epilepsy

Number of pages: 22 pages including this page

Number of words: 200 words in abstract, 5,047 words in the main body

Number of figures: 6 color figures in the main munuscript, 4 color figures in the supplementary information

Number of tables: 1 table in the main manuscript and two tables in the supplementary information

Highlights

- TMS-EEG allows probing of human brain excitability and functionality in health and disease.
- Tensor decomposition to identify key features of high-dimensional EEG data.
- Using this data-driven approach, we reveal the effects of antiepileptic drugs on TMS-EEG.

Abstract

Transcranial magnetic stimulation combined with electroencephalography is a powerful tool to probe human cortical excitability. The EEG response to TMS stimulation is altered by drugs active in the brain, with characteristic “fingerprints” obtained for drugs of known mechanisms of action. However, the extraction of specific features related to drug effects is not always straightforward as the complex TMS-EEG induced response profile is multi-dimensional. Analytical approaches can rely on *a-priori* assumptions within each dimension or on the implementation of cluster-based permutations which do not require preselection of specific limits but may be problematic when several experimental conditions are tested.

We here propose an alternative data-driven approach based on PARAFAC tensor decomposition, which provides a parsimonious description of the main profiles underlying the multidimensional data. We validated reliability of PARAFAC on TMS-induced oscillations before extracting the features of two common anti-epileptic drugs (levetiracetam and lamotrigine) in an integrated manner.

PARAFAC revealed an effect of both drugs, significantly suppressing oscillations in the alpha range in the occipital region. Further, this effect was stronger under the intake of levetiracetam.

This study demonstrates, for the first time, that PARAFAC can easily disentangle the effects of subject, drug condition, frequency, time and space in TMS-induced oscillations.

1. Introduction

Transcranial magnetic stimulation (TMS) is a non-invasive tool to probe neurophysiological processes in the human brain. A TMS pulse depolarizes the stimulated neuronal population and remote anatomically connected regions [1]. The registration of TMS effects with electroencephalography (EEG) allows to quantify and characterize spread of neural activation that follows in time, spatial and frequency domains [2]. The summation of synaptic potentials produces a series of time-locked positive and negative deflections visible in the EEG signal, termed the TMS-evoked potentials (TEPs). TEPs are a sequence of peaks which reflect cortical reactivity and changes in their amplitude and latency reflect changes in cortical activity [3]. In addition, brain responses to TMS can be interrogated applying a time-frequency analysis at single trial level removing the evoked (i.e. TEPs) component from the signal. TMS-induced oscillations are the result of this analytical approach and they provide non-phase locked neural information [4].

TEPs and TMS-induced oscillations are outcome measures used to characterise brain states in health, diseases and under experimental conditions such as drug manipulation [5]. Previous work showed that TMS-EEG is a powerful tool to investigate effects of drugs acting in the human brain [6-10]. In these studies, the effects of drugs were quantified in term of differences between conditions (or subjects) in evoked activity in specific time windows corresponding to TEPs and in specific sets of EEG electrodes. A cluster based permutation approach is the golden standard used to overcome the problem of multiple comparisons. It requires an a-priori selection of time windows or a post-hoc correction for the large number of non-independent comparisons across many tested conditions. It seems highly likely that important effects will be lost through inadvertent selection of the “wrong” time windows and/or electrodes, or through the necessarily harsh post-hoc correction for multiple non-independent comparisons.

The high dimensionality of TMS-EEG data is a challenge for analysis and interpretation, and motivates approaches to simplify the data by reducing the dimensionality. Specifically, we can hypothesise that TMS stimulation of the brain gives rise to activity in specific brain networks following stimulation, and that these networks will have a specific spatial distribution and specific spectral characteristics (i.e. the network operates in a particular frequency range) –

but identifing such underlying patterns in highly multidimensional data is difficult. Here, we apply a methodology based on tensor decomposition to reveal such underlying patterns.

The term "tensor" refers to a multi-way (i.e. multidimensional) array, that is a collection of variables that can be indexed by more than two terms. Whereas the position of and element in a vector or matrix is determined, respectively, by one (e.g., *i*) or two indices (e.g., *i*,*j*) , the values in a tensor are indexed by more than two parameters: *i*, *j*, *k* [11]. In a similar way to how matrix decompositions (e.g., principal component analysis) can represent a two-dimensional array (a matrix) as a product of factor matrices, tensor decompositions allow us to extract from seemingly complex multidimensional data parsimonious and unique representations of underlying patterns [11,12]. Since the introduction of the PARAFAC algorithm, which decomposes a tensor into a sum of outer products of low-rank components [13], tensor decompostions, and PARAFAC in particular, have been used in a wide range of studies of EEG activity [14]. Seminal studies focused on the analysis of event-related potentials [15,16]. Subsequent tensor decompositions of EEG data enabled the inspection of time-frequency representations of EEGs during cognitive states [17]. Tensor decomposition has also been used in artefact rejection and estimation of seizure onset zone [18,19]. Other applications include localisation of EEG sources [20], connectivity estimation [21], brain computer interfaces [22,23], and feature extraction in clinical and psychological studies [24-26]. Tensor decomposition are also useful when fusing EEG with other datasets [27-29]. Overall, the use of tensor decompositions is advatageous over matrix factorisations when the data are naturally multdimensional like in the case of EEG, and TMS-EEG [12].

In this study, we sought to apply a data-driven approach, exploting the multidimensional structure of previously collected TMS-EEG data, allowing a parsimonious dimensionality reduction that summarises effects in the high-dimensional data. We hypothesise that PARAFAC will be able to reveal underlying patterns of activity with different topographical (accounting for the spatial distribution of a brain network), temporal (indicating time period after TMS stimulation during which the network is active) and spectral (informing about the typical operating frequency of the network) profiles that will be characteristic of the effects of each type of anti-epileptic drug (AED) in the TMS-EEG data without a-priori assumptions.

2. Methods

2.1 Subjects

Thirteen healthy male volunteers aged 19-34 years (mean age 25.2 years, SD = ± 4.62) participated in the study after written informed consent was given. All subjects were classified as right-handed according to the Edinburgh Handedness Inventory [30] and underwent physical examination and screening for any contraindications to TMS or study drugs [31]. The College Research Ethics Committee (CREC) of King's College London approved the research, which was performed in accordance with relevant guildlines and regulations. Informed consent was obtained from all participants. The TMS-evoked EEG potential (TEP) analyses of this sample have been published previously [7,32].

2.2 Experimental design

We performed a double-blind, randomized, placebo-controlled, crossover study to investigate the impact of levetiracetam (LEV, 3000 mg) and lamotrigine (LTG, 300mg) on TMS-induced EEG oscillations. Each subject participated in three experimental sessions in total, administered lamotrigine, levetiracetam or placebo in each session in a randomized order, spaced at least one week apart to allow a washout period. At each session, we first performed baseline pre-drug TMS-EEG recording. Later, the post-drug recording was performed two hours after drug ingestion, please see the details of the experimental setting and protocol in the supplementary section A.1.

2.3 Data analysis

2.3.1 TMS-EEG data construction

TMS-induced oscillations were analysed using MATLAB® (Mathworks Ltd, USA, R2012b) (The Mathworks Inc.) and FieldTrip toolbox [33]. After excluding records/trials with prominent eye movements, blinks, and muscle artefacts (on the basis of visual inspection), EEG data was analyzed using an established multistep procedure [34]. Data was down sampled to 1 kHz, segmented 1 s before and after the pulse, and linearly interpolated for ±10 ms to remove the TMS artefact. Bad channels were removed from the EEG, and the signal was reconstructed by interpolating the surrounding electrode signals. Data was then notched filtered (50 Hz). Independent Component analysis (ICA) was applied to remove TMS-related artifacts (i.e., the

cranial muscle response, the recharging of capacitors, and related exponential decay artifacts [35-37], as well as further muscle and ocular activity. Finally, remaining data were re-referenced to the average of all electrodes, baseline corrected (from -1000 to -50 ms) and band-pass filtered (1-80 Hz).

After that, for each segment we estimated its time-frequency plot by applying a Hanning taper windowed fast Fourier transform (FFT) with frequency-dependent window length (width: 3.5 cycles per time window, time steps: 10 ms, frequency steps: 1 Hz from 4 to 45 Hz) [38]. TMS-induced responses were obtained by subtracting the individual time-domain average from each trial before calculating the TF of the single trials [39]. We performed single-trial normalization by z-transforming the TF of each trial for each frequency. The z-transformation was based on the respective mean and standard deviation derived from the full trial length. This was followed by an absolute baseline correction for each trial, by subtracting the average of the 100 to 50 ms period for each frequency to ensure z-values represented a change from pre-TMS baseline.

At the end, we had an array of 61 x 42 x 201 elements (61 channels, 4 Hz to 45 Hz with frequency resolution of 1Hz, and data starting from -1000 to +1000 ms with time step of 10 ms). Note that, to minimise TMS and DC shifts effects along the time (3rd dimension) and frequency (2nd dimension) axes, we selected the data starting from 40 ms after the TMS pulse to 1000 ms after the TMS pulse and frequency bins between 4 to 34 Hz resulting in a new 3D array of 61 × 31 × 98 elements. These steps were repeated for all segments and all channels.

2.3.2 Tensorisation of TMS-EEG data and PARAFAC modelling

The TMS-EEG data construction described in section 2.3.1 resulted in a three dimensional tensor [channel (or space) × frequency × time], representing a time varying spectrum of all channels. Tensors are multi-dimensional data arrays that extend vectors (one dimensional) and matrices (two dimensional) to more than two dimensions [11,12]. This three-dimensional tensor [channel (or space) × frequency × time] will be used in our subsequent tensor decomposition based analysis. Figure 1 illustrates the principle of tensor decomposition based on the PARAFAC model for our tensorised TMS-EEG data (as a 3D tensor for simplicity).

Assuming that we have a 3D tensor **W**, this data array can be approximated as a sum of *N* rank-one tensors, which represent underlying components [17,40]. Each component is an outer product of three matrices (**A**, **B** and **C**) as:

$$w_{ijk} \approx \sum_{r=1}^{n} a_{ir} \cdot b_{ir} \cdot c_{ir}, \qquad (1)$$

where w_{ijk} is an element in the tensor **W**, which is approximated by the summation of *N* rank-1 components which are the outer product of $a_{ir} \cdot b_{ir} \cdot c_{ir}$, where, for example, a_{ir} is an element in the matrix **A** which contains the profiles of the extracted components along the first dimension (channel or space). Likewise, **B** and **C** contains the estimated components along the second (frequency) and third (time), respectively, see Figure 1 (A and B). This data model assummes that the neural generators resulting in the scalp EEG activity are stationary during the recording period.

2.3.3 Selecting the optimum number of components

There is no a priori means to determine how many components will best represent the data. Explained varinace were used to help estimate an appropriate number of components in PARAFAC.

To estimate the optimal number of components, we decomposed a 5D tensor (consisting of all conditions from all subjects [61 × 31 × 98 × 13 × 6 elements]) into a different number of components ranging from one to eight (*n=1,..,8* in equation 1), and estimated the explained variance in each instance. The selection of a relatively low number of components reduces the chances of overfitting and faciltiates its intepretation. More importantly, the topographical, temporal and spectral profiles of the extracted components were inspected to determine a number of PARAFAC components that would aid in the interpretation of the data. It is important to inspect the profiles of components extracted for each considered value of *n* since it is not guaranteed that the components extracted when computing PARAFAC with *n*–1 will appear again when doing so with *n* components [13].

Besides estimating the explained varaince, we also estimated the core consistency diagnosis (CORCONDIA, see the supplementary section A2) [41]. CORCONDIA is a heuristic measure to check if the data can be modelled fully multilinearly.

2.3.4 Using tensor decomposition to characterise and contrast effects of AEDs and placebo

Building on the 3D tensor described above, we constructed a five dimensional tensor consisting of the three previously described dimensions (space, frequency, time) and adding two further dimensions, subject and condition (see Figure 2), by stacking 3D tensors obtained from section 2.3.2 in order to account for all the interactions of space, time and EEG oscillation frequency with the effects of drugs on the subjects. We then tested the effects of drugs on the subjects by contrasting conditions in four different ways, and including these conditions in the 5th dimension (condition):

Model 1: We also use this model as a proof of concept to study the components obtained from PARAFAC without any effect from drug in order to validate the tensor decomposition of TMS-EEG data.

Model 2: To test the hypothesis that levetiracetam and lamotrigine have different effects, we included four conditions: pre-LEV, post-LEV, pre-LTG, post-LTG.

Model 3: To test the hypothesis that levetiracetam has a different effect than placebo, we included four conditions: pre-placebo, post-placebo, pre-LEV, post-LEV.

Model 4: To test the hypothesis that lamotrigine has a different effect than placebo, we included four conditions: pre-placebo, post-placebo, pre-LTG, post-LTG.

These four separate models allow us to first validate the application of PARAFAC to TMS-EEG data and then to compare in pairs the effect of each drug between them and versus placebo in data-driven, unsupervised way. Considering the post processed data (3D tensors) obtained from step 2.3.2, for each subject (per condition) we had a data array of 61 × 31 × 98 elements. After stacking these 3D tensors from all subjects for the specific conditions as described in each model, we obtained a 5D tensor of 61 × 31 × 98 × 13 × 4 elements. Unlike the example in Figure 1, showing the decomposition of the 3D tensor, with the newly constructed 5D tensor we could decompose this 5D array into a sum of 5 rank-one tensors (space (or channel), frequency, time, subject, and condition).

In this study, we used the N-way toolbox version 3.3 for tensor decomposition [42] (http://www.models.life.ku.dk/nwaytoolbox). Note that we applied the non-negativity constraint to all dimensions while performing decomposition. Thus every element in the

decomposed arrays would be at or greater than zero [14,17,43]. This constraint was imposed for a ease of interpretation.

2.3.5 Statistics

We applied a permutation based analysis to test for significant difference between pre-vs-post drug. All steps taken are presented as follows (see the graphical representation of all the steps in the supplementary Figure A1). At each model, we first decomposed the 5D tensor (with 61 x 31 x 98 x 13 x 4) into three components. These components were considered as 'master' components (that is, the 'true labelled' components, in distinction to permuted components, see below). Each of these components consisted of five profiles across the five dimensions (axes). For example in model-1, at each component we obtained five rank-1 tensors with 61, 31, 98, 13, and 4 elements for space, frequency, time, subject and condition, respectively.

Then we permuted this 5D tensor for 1,000 iterations. At each iteration, we permuted the elements on the 4^{th} and 5^{th} dimensions (subjects and conditions). Next, we decomposed this permuted 5D tensor while fixing all elements in the first three tensors. From this step, we obtained a new set of five rank-1 tensors, where thre first three tensors (representing space, frequency and time) were similar to the ones in the master, but the elements in the 4^{th} and 5^{th} tensors could be different from the master because shuffling the data along those dimensions destroys the inherent structure.

To assess the effects after drug/placebo intake, we subtracted the value on the 5^{th} dimension of the pre drug from the value post drug. For example, considering the 2^{nd} component of the master (true label), we subtracted the value before LEV intake from the value after LEV intake see the supplementary Figure A1). For the permuted data, at each iteration we estimated the level of change post drug as we did with the master. Then, we computed a histogram of these values. The level of change in master (true label) was significant if its value was less (or greater) than 2.5% of the distribution of the histogram. Note that the green square in the histogram at the bottom tight of the supplementary Figure A1 represents the difference between pre-vs-post LEV, where the two red vertical lines represent the upper and lower 2.5% of the histogram.

2.4 Data and code availability statement

Data and code are available upon request.

3. Results

3.1 Optimum number of decomposed components

We first explored our data to determine the optimal number of components. We decomposed the 5D tensor (space, frequency, time, subject, condition) build from all subjects and all six conditions into a range of number of components from one to eight. First, we showed the percentage of explained variance at different number of components in Table 1. Then, we showed the topographical, temporal and spectral profiles of the extracted components from all eight cases (see the supplementary Figures A2-A4).

From Table 1, a marked change was found in these parameters when increasing the number of components from one to three: i.e. ~10% increase in terms of explained variance. Above 4 components, further increasing the number of components did not significantly change either of these parameters.

In the supplementary Figure A2, representing the decomposed components on the 1st dimension (space), we found three typical underlying spatial patterns (highlighted in green, red and blue), which were relatively consistent (at least 6 out of 8 scenarios).

Moving on to the frequency axis (2nd dimension), if we decomposed the 5D tensor into a single component, this component would be represented primarily in the alpha range, see the supplementary Figure A3. When decomposing the same 5D tensor into two components, a component primrily in the theta frequency range was found in addition to the alpha component. Decomposed into three components, we observed they were distinct, primarily in theta, alpha and beta bands. After that, increasing the number of components did not add any other distinct components at other frequency bands, as most of the further decomposed components overlapped with the components found when decomposed into just three.

Finally, in the time axis unlike the first two axes it was harder to justify a number of independent components. By visual inspection, at least three distinct components were found, see the supplementary Figure A4.

Taking these together, we decided to decompose the 5D tensor into three components where the three distinct frequency band and three unique spatial patterns were clearly observed and the explained variance reached its plateau at about 40%.

3.2 Comparison across the four models

Figure 3 shows three components decomposed from our four different models. The 5D tensor from each model was decomposed into three components at three different frequency bands (theta, alpha, and beta, see the 2nd column in Figure 3).

The model 1 is a proof of concept showing the three physiological components (beta, alpha and theta) decomposed from the TMS-EEG data without any effect from LEV or LTG.

First considering the beta components (labelled in blue) from all models, these components mostly represented frontal brain activities. On the time axis (3rd dimension), each of these beta components could be divided into 3 phases: (1) initial peak (during 40 – 200 milliseconds), (2) suppression (200 – 400 milliseconds) and (3) rebound (400 milliseconds onward). When we compared between models 3 and 4 (between LTG and LEV), one could observe less rebound of this beta component in LTG as compared to LEV.

The next component, which was predominantly observed in alpha range, showed the most variability (in terms of magnitude and spatial pattern) among the three components (theta, alpha, and beta) across all models. Whereas one could see the alpha component dominating occipital lobe in models 2 and 3, in model 4 this alpha activity can be seen everywhere (with high amplitude) except on the areas next to the earlobes.

Moving on to the last component, or theta labelled in orange, it was spatially identical across all models and represented the activities on C3. This component reached its peak around 200 milliseconds and completely suppressed starting ~400 milliseconds to the end of each recording.

3.3 Model 2: comparison of the effects of levetiracetam and lamotrigine.

Figure 4 shows the three decomposed components in five dimensions, which were highlighted in blue, red and orange for 1st, 2nd and 3rd components respectively. The first component (blue) represented the brain activities (in the beta range, peak at 19 Hz) over the frontal and central areas. On the time axis (3rd dimension), this component initially peaked at

~90 milliseconds after applied TMS pulse, then suppressed between 190 – 400 milliseconds, and rebounded from 440 milliseconds to the end of the recording.

The second component (red) represented the activities with relatively lower frequency (at alpha band or between 6 - 13 Hz), which predominantly involved the occipital lobe. Initially, during 40 – 140 milliseconds after the TMS pulse, while the 1st component (frontal beta) was reaching its peak, this component (occipital alpha) was absent. Subsequently, during 140 – 340 seconds, while the 1st component was declining and eventually completely diminished, this 2nd component was on the rise and reached a plateau. Starting from 440 milliseconds until the end of the recording, these two components coexisted.

The last component (3rd, orange) was found in the theta band (4-6 Hz), centered on EEG electrode C3, which was the location where the TMS pulses were given. This component reached its peak between 90 – 240 milliseconds, and later was suppressed starting from 440 milliseconds until the end of recording (which was the period where both 1st and 2nd components coexisted).

Inter-subject variabilities were revealed in the 4th dimension showing the 1st , 10th and last subject being different from the others. On the 5th dimension condition (drug) effects were revealed, and we observed reduction in all components after receiving medication (both LEV and LTG). From this plot, one could see a stronger post medication effect for LEV as compared to LTG, especially in the 2nd component. At a group level, there was a significant effect of reduction of the 2nd component after LEV intake (see Figure 5).

3.4 Statistics

Figure 6 shows distributions of difference between pre-and-post medication from 1000 iterations in models 2, 3 and 4. Statistically, no significant change in either theta or beta components was found (see columns 1 and 3). Considering models 3 and 4, when we investigated the effects after drug vs after plecebo, we found significant reduction of alpha component in both post LEV ($p=0.015^*$) and post LTG ($p=0.021^*$) conditions. In model 2, when we compared the effects after drug intakes in both LEV vs LTG, the post-LEV shows a significantly stronger reduction of the alpha component than post-LTG with $p=0.01^*$.

4. Discussion

In this study, we introduced a tensor decomposition method to reduce multi-dimensionality of TMS-EEG data. We showed a series of components which provides a parsimonious description of neurophysiological responses underlying TMS-induced oscillations. In addition we demonstrated the utility of PARAFAC on existing data to disentangle the effect of anti-epileptic drugs on TMS-indueced oscillations. This method does not require *a-priori* selection of anatomical regions of interest, time periods of interest and frequency components of interest in the multi-dimensional EEG data, and without requiring potentially harsh post-hoc statistical correction for multiple comparisons. PARAFAC revealed an effect of both levetiracetam and lamotrigine, significantly suppressing oscillations in the alpha range in the occipital region, during the time period approximately 140 ms - 840 ms after the TMS pulse. Furthermore, this technique also reveals that the suppression of alpha oscillations is significantly stronger during the intake of levetiracetam than lamotrigine.

4.1 Optimum number of decomposed components and justification of PARAFAC model

From Table 1, the explained variance in the data reached its plateau when splitting into three components. This suggsests three as the optimal components. To justify our choice, we also visually inspected the decomposed profiles on space, time and frequency axes (supplementary Figures A2 – A4). This is important as the profiles of components extracted for each considered value of n since it is not guaranteed that the components extracted when computing PARAFAC with *n*–1 will appear again when doing so with *n* components [13]. The fact that similar patterns appeared naturally provides further support to the interpretability of our chosen model. The inspection of the components also enabled us to grasp which physiological processes captured by the data-driven components were prominent in the TMS-EEG recordings. The results support our choice of 3 components. It was clear that along the frequency axis (supplementary Figure A3) regardless of the number of decomposed components we could only break down into maximum three different frequency bands (theta, alpha, and beta). Moving on to the spatial axis (the supplementary Figure A2), it was debatable if a maximum number of components could be either three or four. Finally, along the time axis (the supplementary Figure A4), the optimal number of component was unclear (it could either be any number between two to four). Looking at the CORCONDIA in the supplementary Table A2, we found that by extracting more than one component the value of

CORCONDIA drop to zero. This suggests our 5D tensor is not a fully multilinear form and also explains the non-equivalent number of optimal components along different axes [41]. Taking all these together, we then decided to decompose into three components, where all three unique signatures along frequency and spatially domains were found, and the explained variances reached its plateau. It is important to note that the explained variance may not increase significantly with the number of components since the multilinear PARAFAC model will not explain the noise and random variations in the data. Furthermore, increasing the number of components would lead to higher computational cost [44].

Although another family of tensor decompositions (Tucker decompositon) may provide a solution to the case with a non-equivalent number of optimal components, it does not preserve one-to-one interaction [33,45]. Hence, the decomposed components using Tucker decomposition are harder to interpret. To sum up, we decided to decompose the TMS-EEG 5D tensor using PARAFAC, which preserves one-to-one interaction. That is each component will be entitled to a unique interpretation, for example, the TMS induced component may be seen in a particular frequncy range, anatomical distribution and time period. Future work will explore the suitability of other more flexible, but still unique models such as PARAFAC2 [21], to improve the modelling of TMS-EEG data and reveal even more subtle interactions.

4.2 Physiological meanings behind the three components

From model 1 (without drug) we found three physiological components (theta, alpha and beta), these components are highly similar (spatially, temporally and spectrally) across four models, see Figure 3. Given that the PARAFAC solution is unique under very mild conditions, this further reinforces that the extracted components have physiological meaning. These components (frontal-sensorimotor beta, posterior alpha and theta related to the site of stimulation) represented the hidden signature of the data for all conditions (pre/post PLA, pre/post LEV, pre/post LTG). We considered the frontal-sensorimotor beta component to represent the spreading of cortical reactivity from the stimulated site (C3) through its neighboring areas via local fibers as well as to the contralateral motor cortex via corpus callosum [46]. Sensorimotor rhythms, which dominate the motor cortex, are found in mu (8-13 Hz) and beta rhythms (15-30 Hz) [47,48]. By giving a TMS pulse, it may elicit similar effects on the cortical neurons seen as event-related (de)-synchronization (ERD/ERS) time locked to motor movement over motor cortex areas [49-51]. Since the rebound of sensorimotor rhythms

(synchronization) is uniquely observed in the beta range after giving stimuli [49,50], by imposing the non-negativity constraint to the 5D tensor we might limit the decomposed component at this area only in the beta band. Moving on to the posterior alpha, it is found to be a key component shown to differentiate between the two drugs, seen as the stronger reduction of alpha component after LEV compard to LTG intake, in model 2. Considering both models 3 and 4 (placebo vs each type of drug), we found the significant reduction of this component after both LEV and LTG intake (whereas no change was found post placebo). Results suggest that both types of drug cause similar effects on the generation of posterior alpha. The same observation derived from the investigation of these AEDs on TEPs, where despite the varying profile of effects and regardless of the (putative) molecular targets of the different drugs, systemically administered LEV and LTG exert similar modulation of TEPs (Premoli et al 2017). In addition, the effect on alpha was stronger under LEV exposure which had the highest average concentration in blood outside the reference range, with LTG averaging toward a lower concentration for its reference range (Premoli et al 2017).

Lastly, considering theta, this component represents the TMS-induced effect on the stimulation site, because its spatial pattern was centred on C3 and its temporal signature shows a peak soon after stimualtion and then subsided.

4.3 Strengths and weaknesses of this study

Unlike a conventional TMS-EEG analysis, which requires predefining time, anatomical area and frequency of interest, tensor decompositions offer a purely data-driven approach. In particular, we applied PARAFAC due to its parsimony and ease of interpretation since the interactions of the components are restricted. In our analysis, the 5D tensor for each mode had dimensions 61 × 31 × 98 × 13 × 4 (9,636,536 entries in total). Decomposing it with PARAFAC, the method was able to account for approximately 40% of the explained variance with just 3 components which include only 621 elements – i.e., 3 × (61 + 31 + 98 + 13 + 4), less than 0.01% of the total number of entries in the tensor. The results were tested under permutation-based statistics. We successfully showed that each decomposed component represents the unique signature on the spatial, spectral and temporal domains with physiological meaning. Furthermore, along the 4th dimension, one could make the inference

about these hidden signatures at a single subject level. Despite the postive results provided by this innovative analysis approach of TMS-EEG data, it must be take into consideration that the TMS pulse can induce unwanted somatosensory input that have an impact on TEPs [52]. We purposely selected a PARAFAC model with non-negativity constraints to simplify the interpretation of the components extracted from TMS-EEG activity in this first application of tensor decompositions to this type of data. However, we acknoledge that the choice of the non-negativity constraint implies that we were not able to reveal potential patterns in negative values and that our results are also limited by the small number of participants and we advice the reader to intepret them with care.

5. Conclusion

To our knowledge, it is the first time tensor decomposition has been applied in TMS-EEG data. Our results show the power of tensor decompositions to reveal the profiles underlying the complex responses in TMS-EEG data associated with different AEDs in healthy subjects in a data-driven and parsimonious way. Future work will seek to develop classifiers able to predict the level of response to each AED in new subjects by projecting their TMS-EEG recordings on the "characteristic filters" associated with previously revealed tensor components in space, time and frequency [26,53]. We will also consider the possibility of applying tensor decompositions to TMS-EEG signals in the time domain following other previous applications of these techniques to event-related EEG activity [14].

Acknowledgements

JE acknowledges support by EPSRC, UK, under Grant EP/N014421/1 and from an RS MacDonald Seedcorn Award. MPR is funded by MRC Programme Grant MR/K013998/1, EPSRC Centre for Predictive Modelling in Healthcare EP/N014391/1, and by the NIHR Biomedical Research Centre and South London and Maudsley NHS Foundation Trust and King's College London.

Contributions

MR, JE and RC designed and supervised the research. IP collected and preprocessed the data. CT and LS wrote the analysis scripts. CT analysed the data. CT, IP and JE wrote the manuscript. All authors reviewed the manuscript.

Conflicts of interest

The authors declare that there is no conflict of interest.

References

1 Hallett, M. Transcranial magnetic stimulation: a primer. *Neuron* **55**, 187-199, doi:10.1016/j.neuron.2007.06.026 (2007).

2 Ilmoniemi, R. J. *et al.* Neuronal responses to magnetic stimulation reveal cortical reactivity and connectivity. *Neuroreport* **8**, 3537-3540 (1997).

3 Rogasch, N. C. & Fitzgerald, P. B. Assessing cortical network properties using TMS-EEG. *Hum Brain Mapp* **34**, 1652-1669, doi:10.1002/hbm.22016 (2013).

4 Rosanova, M. *et al.* Natural frequencies of human corticothalamic circuits. *J Neurosci* **29**, 7679-7685, doi:10.1523/JNEUROSCI.0445-09.2009 (2009).

5 Tremblay, S. *et al.* Clinical utility and prospective of TMS–EEG. *Clinical Neurophysiology*, doi:10.1016/j.clinph.2019.01.001 (2019).

6 Darmani, G. *et al.* Effects of the Selective alpha5-GABAAR Antagonist S44819 on Excitability in the Human Brain: A TMS-EMG and TMS-EEG Phase I Study. *J Neurosci* **36**, 12312-12320, doi:10.1523/JNEUROSCI.1689-16.2016 (2016).

7 Premoli, I., Biondi, A., Carlesso, S., Rivolta, D. & Richardson, M. P. Lamotrigine and levetiracetam exert a similar modulation of TMS-evoked EEG potentials. *Epilepsia* **58**, 42-50, doi:10.1111/epi.13599 (2017).

8 Darmani, G. *et al.* Effects of antiepileptic drugs on cortical excitability in humans: A TMS-EMG and TMS-EEG study. *Hum Brain Mapp* **40**, 1276-1289, doi:10.1002/hbm.24448 (2019).

9 Premoli, I., Biondi, A., Carlesso, S., Rivolta, D. & Richardson, M. P. Lamotrigine and levetiracetam exert a similar modulation of TMS-evoked EEG potentials. *Epilepsia*, doi:10.1111/epi.13599 (2016).

10 Premoli, I. *et al.* TMS-EEG signatures of GABAergic neurotransmission in the human cortex. *J Neurosci* **34**, 5603-5612, doi:10.1523/JNEUROSCI.5089-13.2014 (2014).

11 T.G. Kolda, B. W. B. Tensor Decompositions and Applications. *SIAM Reviews* **51**, 455-500 (2009).

12 Cichocki, A. *et al.* Tensor Decompositions for Signal Processing Applications. *Ieee Signal Processing Magazine* **32**, 145-163, doi:10.1109/Msp.2013.2297439 (2015).

13 Harshman, R. A. Foundations of the PARAFAC procedure: Models and conditions for an —explanatory" multimodal factor analysis. *UCLA Working Papers in Phonetics* **16**, 1-84 (1970).

14 Cong, F. Y. *et al.* Tensor decomposition of EEG signals: A brief review. *Journal of Neuroscience Methods* **248**, 59-69, doi:10.1016/j.jneumeth.2015.03.018 (2015).

15 Cole, H. W. & Ray, W. J. Eeg Correlates of Emotional Tasks Related to Attentional Demands. *International Journal of Psychophysiology* **3**, 33-41, doi:Doi 10.1016/0167-8760(85)90017-0 (1985).

16 Mocks, J. Decomposing Event-Related Potentials - a New Topographic Components Model. *Biological Psychology* **26**, 199-215, doi:Doi 10.1016/0301-0511(88)90020-8 (1988).

17 Miwakeichi, F. *et al.* Decomposing EEG data into space-time-frequency components using Parallel Factor Analysis. *Neuroimage* **22**, 1035-1045, doi:DOI 10.1016/j.neuroimage.2004.03.039 (2004).

18 Acar, E., Aykut-Bingol, C., Bingol, H., Bro, R. & Yener, B. Multiway analysis of epilepsy tensors. *Bioinformatics* **23**, i10-18, doi:10.1093/bioinformatics/btm210 (2007).

19 De Vos, M. *et al.* Canonical decomposition of ictal scalp EEG reliably detects the seizure onset zone. *Neuroimage* **37**, 844-854, doi:10.1016/j.neuroimage.2007.04.041 (2007).

20 Becker, H. *et al.* EEG extended source localization: tensor-based vs. conventional methods. *Neuroimage* **96**, 143-157, doi:10.1016/j.neuroimage.2014.03.043 (2014).

21 Spyrou, L., Parra, M. & Escudero, J. Complex Tensor Factorization With PARAFAC2 for the Estimation of Brain Connectivity From the EEG. *IEEE Trans Neural Syst Rehabil Eng* **27**, 1-12, doi:10.1109/TNSRE.2018.2883514 (2019).
22 Cichocki, A. *et al.* Noninvasive BCIs: Multiway Signal-Processing Array Decompositions. *Computer* **41**, 34-+, doi:Doi 10.1109/Mc.2008.431 (2008).
23 Zhang, Y. *et al.* L1-regularized Multiway canonical correlation analysis for SSVEP-based BCI. *IEEE Trans Neural Syst Rehabil Eng* **21**, 887-896, doi:10.1109/TNSRE.2013.2279680 (2013).
24 Wang, J. *et al.* Characteristics of evoked potential multiple EEG recordings in patients with chronic pain by means of parallel factor analysis. *Comput Math Methods Med* **2012**, 279560, doi:10.1155/2012/279560 (2012).
25 Cong, F. *et al.* Benefits of multi-domain feature of mismatch negativity extracted by non-negative tensor factorization from EEG collected by low-density array. *Int J Neural Syst* **22**, 1250025, doi:10.1142/S0129065712500256 (2012).
26 Latchoumane, C. F. *et al.* Multiway array decomposition analysis of EEGs in Alzheimer's disease. *J Neurosci Methods* **207**, 41-50, doi:10.1016/j.jneumeth.2012.03.005 (2012).
27 Martinez-Montes, E., Valdes-Sosa, P. A., Miwakeichi, F., Goldman, R. I. & Cohen, M. S. Concurrent EEG/fMRI analysis by multiway Partial Least Squares. *Neuroimage* **22**, 1023-1034, doi:10.1016/j.neuroimage.2004.03.038 (2004).
28 Kinney-Lang, E., Ebied, A., Auyeung, B., Chin, R. F. M. & Escudero, J. Introducing the Joint EEG-Development Inference (JEDI) Model: A Multi-Way, Data Fusion Approach for Estimating Paediatric Developmental Scores via EEG. *IEEE Trans Neural Syst Rehabil Eng* **27**, 348-357, doi:10.1109/TNSRE.2019.2891827 (2019).
29 Karahan, E., Rojas-Lopez, P. A., Bringas-Vega, M. L., Valdes-Hernandez, P. A. & Valdes-Sosa, P. A. Tensor Analysis and Fusion of Multimodal Brain Images. *Proceedings of the Ieee* **103**, 1531-1559, doi:10.1109/Jproc.2015.2455028 (2015).
30 Oldfield, R. C. The assessment and analysis of handedness: the Edinburgh inventory. *Neuropsychologia* **9**, 97-113 (1971).
31 Rossi, S., Hallett, M., Rossini, P. M., Pascual-Leone, A. & Safety of, T. M. S. C. G. Safety, ethical considerations, and application guidelines for the use of transcranial magnetic stimulation in clinical practice and research. *Clin Neurophysiol* **120**, 2008-2039, doi:10.1016/j.clinph.2009.08.016 (2009).
32 Premoli, I., Costantini, A., Rivolta, D., Biondi, A. & Richardson, M. P. The Effect of Lamotrigine and Levetiracetam on TMS-Evoked EEG Responses Depends on Stimulation Intensity. *Front Neurosci* **11**, 585, doi:10.3389/fnins.2017.00585 (2017).
33 Oostenveld, R., Fries, P., Maris, E. & Schoffelen, J. M. FieldTrip: Open source software for advanced analysis of MEG, EEG, and invasive electrophysiological data. *Comput Intell Neurosci* **2011**, 156869, doi:10.1155/2011/156869 (2011).
34 Premoli, I. *et al.* The impact of GABAergic drugs on TMS-induced brain oscillations in human motor cortex. *Neuroimage* **163**, 1-12, doi:10.1016/j.neuroimage.2017.09.023 (2017).
35 Herring, J. D., Thut, G., Jensen, O. & Bergmann, T. O. Attention Modulates TMS-Locked Alpha Oscillations in the Visual Cortex. *The Journal of neuroscience : the official journal of the Society for Neuroscience* **35**, 14435-14447, doi:10.1523/jneurosci.1833-15.2015 (2015).
36 Korhonen, R. J. *et al.* Removal of large muscle artifacts from transcranial magnetic stimulation-evoked EEG by independent component analysis. *Med Biol Eng Comput* **49**, 397-407, doi:10.1007/s11517-011-0748-9 (2011).
37 Rogasch, N. C. *et al.* Removing artefacts from TMS-EEG recordings using independent component analysis: importance for assessing prefrontal and motor cortex network properties. *NeuroImage* **101**, 425-439, doi:10.1016/j.neuroimage.2014.07.037 (2014).
38 Delorme, A. & Makeig, S. EEGLAB: an open source toolbox for analysis of single-trial EEG dynamics including independent component analysis. *J Neurosci Methods* **134**, 9-21, doi:10.1016/j.jneumeth.2003.10.009 (2004).

39 Cohen, M. X. & Donner, T. H. Midfrontal conflict-related theta-band power reflects neural oscillations that predict behavior. *J Neurophysiol* **110**, 2752-2763, doi:10.1152/jn.00479.2013 (2013).
40 Harshman, R. A. Foundations of the PARAFAC procedure: Models and conditions for an — explanatory“ multimodal factor analysis. *UCLA Working Papers in Phonetics* **16**, 1-84 (1970).
41 Bro, R. & Kiers, H. A. L. A new efficient method for determining the number of components in PARAFAC models. *Journal of Chemometrics* **17**, 274-286, doi:10.1002/cem.801 (2003).
42 Andersson, C. A. & Bro, R. The N-way Toolbox for MATLAB. *Chemometrics and Intelligent Laboratory Systems* **52**, 1-4, doi:Doi 10.1016/S0169-7439(00)00071-X (2000).
43 Comon, P., Luciani, X. & de Almeida, A. L. F. Tensor decompositions, alternating least squares and other tales. *Journal of Chemometrics* **23**, 393-405, doi:10.1002/cem.1236 (2009).
44 Sidiropoulos, N. D. *et al.* Tensor Decomposition for Signal Processing and Machine Learning. *Ieee Transactions on Signal Processing* **65**, 3551-3582, doi:10.1109/Tsp.2017.2690524 (2017).
45 Massimini, M. *et al.* Breakdown of cortical effective connectivity during sleep. *Science* **309**, 2228-2232, doi:10.1126/science.1117256 (2005).
46 Voineskos, A. N. *et al.* The role of the corpus callosum in transcranial magnetic stimulation induced interhemispheric signal propagation. *Biol Psychiatry* **68**, 825-831, doi:10.1016/j.biopsych.2010.06.021 (2010).
47 Lopes da Silva, F. Neural mechanisms underlying brain waves: from neural membranes to networks. *Electroencephalogr Clin Neurophysiol* **79**, 81-93 (1991).
48 Neuper, C. & Pfurtscheller, G. Event-related dynamics of cortical rhythms: frequency-specific features and functional correlates. *Int J Psychophysiol* **43**, 41-58 (2001).
49 Pfurtscheller, G., Graimann, B., Huggins, J. E., Levine, S. P. & Schuh, L. A. Spatiotemporal patterns of beta desynchronization and gamma synchronization in corticographic data during self-paced movement. *Clin Neurophysiol* **114**, 1226-1236 (2003).
50 Pfurtscheller, G. & Lopes da Silva, F. H. Event-related EEG/MEG synchronization and desynchronization: basic principles. *Clin Neurophysiol* **110**, 1842-1857 (1999).
51 Brignani, D., Manganotti, P., Rossini, P. M. & Miniussi, C. Modulation of cortical oscillatory activity during transcranial magnetic stimulation. *Hum Brain Mapp* **29**, 603-612, doi:10.1002/hbm.20423 (2008).
52 Conde, V. *et al.* The non-transcranial TMS-evoked potential is an inherent source of ambiguity in TMS-EEG studies. *Neuroimage* **185**, 300-312, doi:10.1016/j.neuroimage.2018.10.052 (2019).
53 Escudero, J., Acar, E., Fernandez, A. & Bro, R. Multiscale entropy analysis of resting-state magnetoencephalogram with tensor factorisations in Alzheimer's disease. *Brain Res Bull* **119**, 136-144, doi:10.1016/j.brainresbull.2015.05.001 (2015).

Table 1: Percentage of explained variance by a number of decomposed components

Scenario	No. of Components	Explained variance (%)
I	1	29.14
II	2	34.06
III	3	39.33
IV	4	41.21
V	5	42.53
VI	6	43.49
VII	7	44.05
VIII	8	44.03

List of Figures

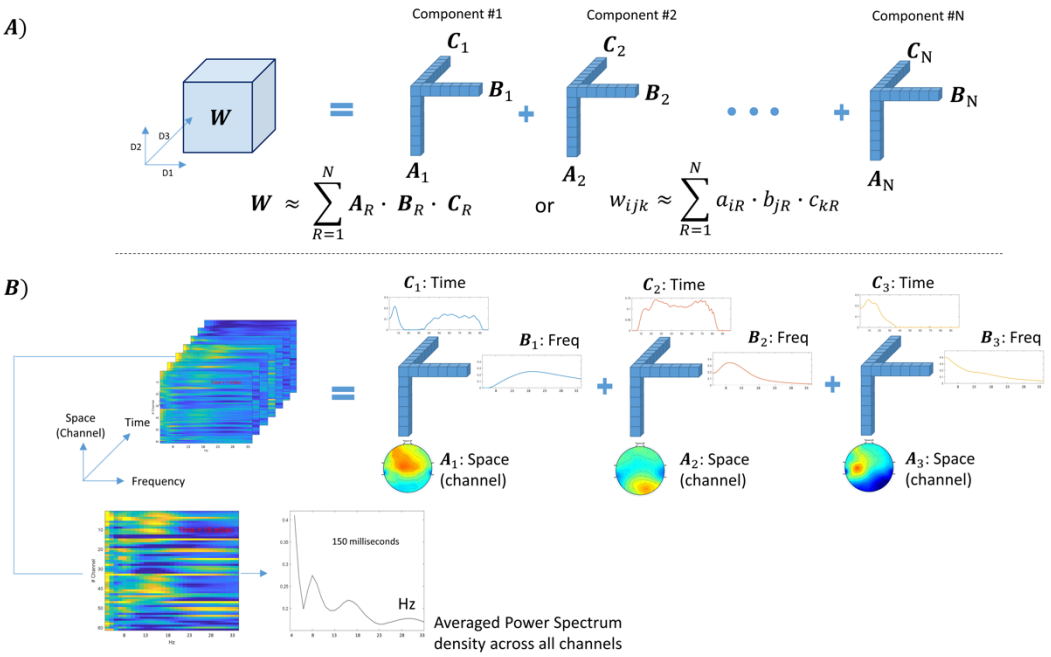

*Figure 1A shows N decomposed components from the 3D tensor **W**, each component comprises three vectors (A, B and C). Figure 1B shows an example when the technique was used to decompose the 3D (space x frequency x time) of subject#2 post LEV. In this case, the three components represent high, medium and low-frequency ranges (15-30 Hz "Beta", 6-13 Hz "Alpha", and 4-6 Hz "Theta". The bottom two insets show a Space-vs-Frequency plot at 150 milliseconds after TMS pulse and its grand average across all channels.*

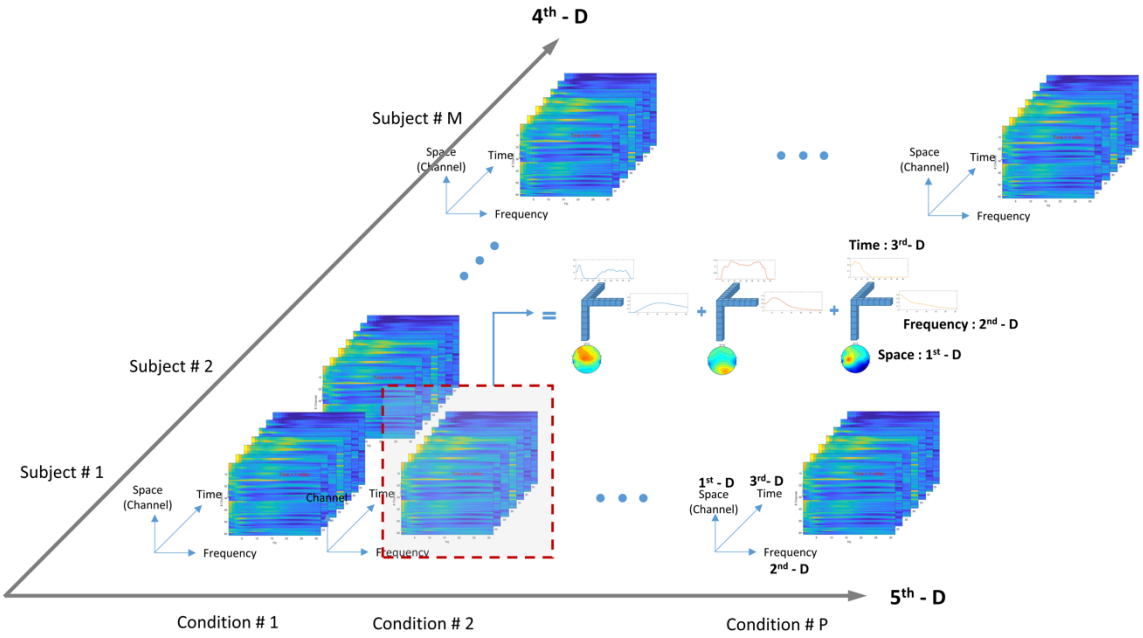

Figure 2: The five-dimensional tensor in this study comprises of space (channel), frequency, time, subject and condition (1st, 2nd, 3rd, 4th and 5th dimension, respectively).

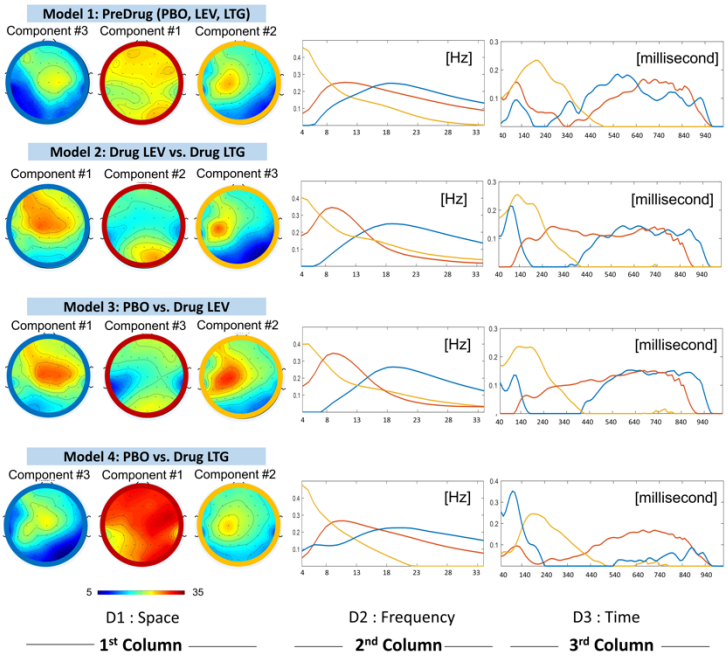

Figure 3: We present the three components decomposed from 5D tensor in four different models. The top row shows the decomposed components in space (topographical plots), frequency and time dimension. Three colours (blue, red and yellow) are used to indicate the three decomposed components: beta (with peak frequency between 15-30 Hz), alpha (with peak frequency between 6-13 Hz) and theta (with peak frequency between 4-6 Hz), respectively.

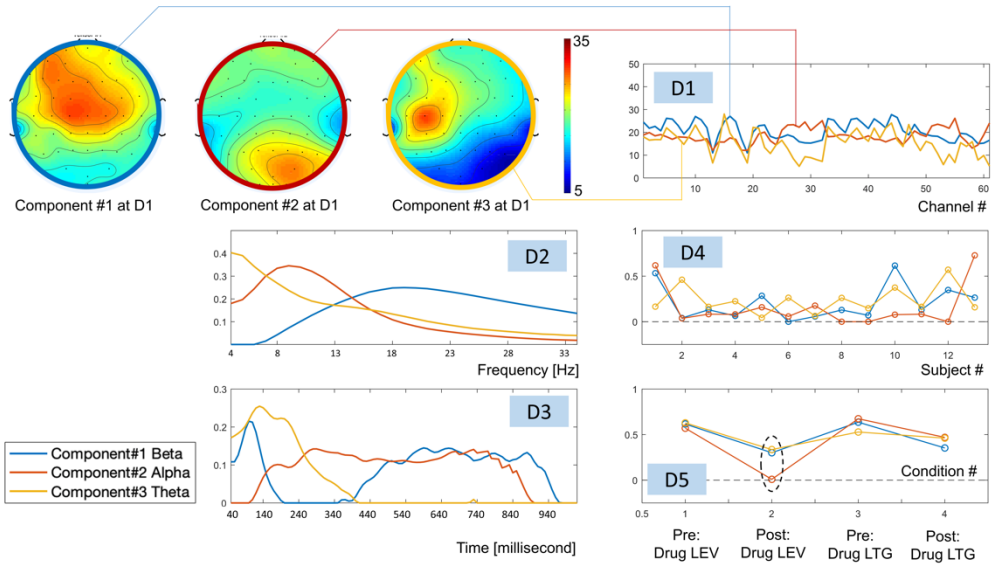

Figure 4: The three components decomposed from the 5D tensor in all subjects during pre-drug and post-drug conditions with LEV or LTG. Note that: D stands for Dimension.

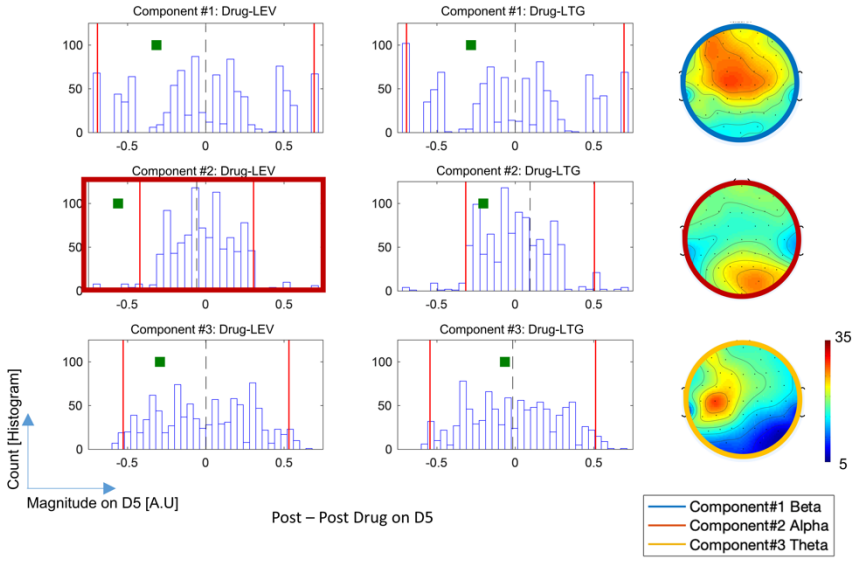

Figure 5: Each histogram shows the distribution of strength on the 5th dimension obtained from 1000 iterations of permutation. Two vertical red lines indicate the upper and lower 2.5% of the histogram. Each green square oindicates the difference between pre and post medication on the 5th dimension. In the top and bottom rows (showing the results from components 1 and 3, respectively), no significant reduction was found. For component #2 (middle row), we observed the significant reduction in terms of strength on the 5th dimension after receiving LEV.

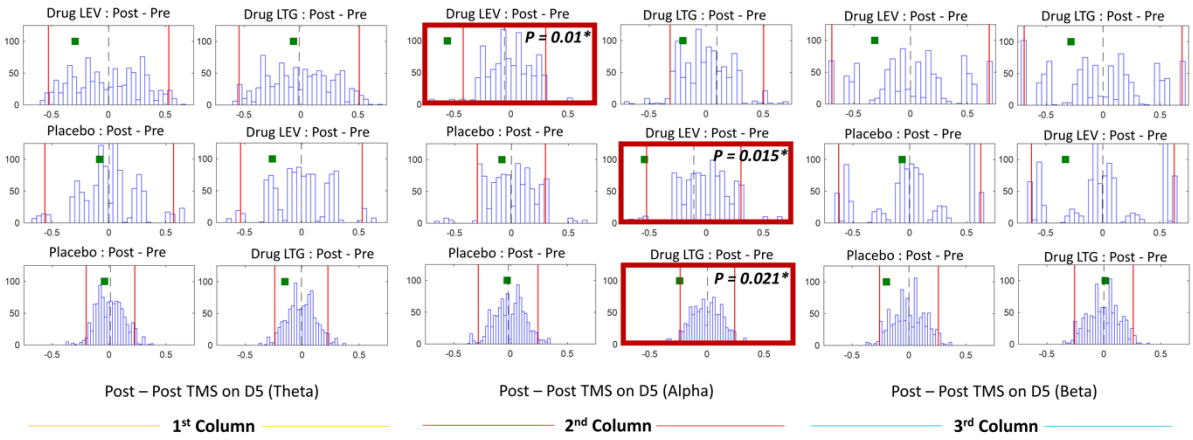

*Figure 6: Each histogram shows the distribution of difference between pre and post medication(or placebo) from 1000 iteration. The two red lines in the histograms indicate the first and last 2.5 percent. The green square represents the post vs pre difference on the 5th dimension. * denotes significant (P<0.025). All histograms on the top, middle and bottom rows are the distribution from model 2, 3, and 4, respectively. Note that all the p-values in this study are reported in the supplementary Table A1.*

Supplementary material

Tensor decomposition of TMS-induced EEG oscillations reveals data-driven profiles of antiepileptic drug effects

Tangwiriyasakul C.[1]*, Premoli I.[1]*, Spyrou, L.[2], Chin R.F.[3], Escudero J[2**], and Richardson M.P.[1**]

[1] Department of Basic and Clinical Neuroscience, Institute of Psychiatry, Psychology and Neuroscience (IoPPN), King's College London, London, UK.

[2] School of Engineering, Institute for Digital Communications, The University of Edinburgh, Thomas Bayes Rd, Edinburgh EH9 3FG, UK

[3] Muir Maxwell Epilepsy Centre, Centre for Clinical Brain Sciences, The University of Edinburgh, West Mains Rd, Edinburgh EH9 3FB, UK

A.1 Extended method

A.1.1 Experimental design

Respective dosages for of leveiracetam (LEV, 3000 mg) and lamotrogine (LTG, 300 mg) were chosen as the most frequently prescribed dose of each medication in patients with epilepsy [1]. Lamotrigine blocks voltage-gated sodium channels, while levetiracetam acts by binding to synaptic vesicle membrane molecule SV2A [2] [3]. Baseline pre-drug TMS-EEG recordings were obtained. Subsequently, participants orally ingested a single dose of either lamotrigine, levetiracetam, or a placebo. Post-drug recordings were performed two hours after drug ingestion and blood samples for plasma drug levels were taken five minutes prior to TMS-EEG testing. Two hours was chosen as an appropriate time period for each drug to reach peak effect after intake, based on their known pharmacokinetics [1]. Each subject participated in three experimental sessions in total, administered lamotrigine, levetiracetam or placebo in each session in a randomized order, spaced at least one week apart to allow a washout period.

A.1.2 TMS-EMG recording

A figure of eight coil (wing diameter 90mm) connected to a Magnetic stimulator (Magstim 200[2]) with a monophasic current wave-form was used to stimulate the left Motor Cortex

(M1). An ideal coil position to produce motor evoked potentials (MEPs) in the first dorsal interosseus (FDI) muscle of the right hand was determined, continuously generating stable responses at amplitude of ∼1 mV TMS. This "hotspot" position and the edge of the coil wing was clearly marked using a pen on the EEG cap.

MEP recordings were obtained through surface EMG, via Ag-AgCl cup-electrodes in a belly-tendon montage. The position of the coil, with the handle pointing backwards over the scalp, away from the midsagittal line, induced a current flow in the lateral-posterior to medial-anterior route which transsynaptically activated the corticospinal system, optimal for eliciting MEPs (Di Lazzaro et al., 2008). Resting motor threshold (RMT) was determined via the application of single TMS pulses, adopting the relative frequency method (Groppa et al., 2012) in a fully relaxed FDI muscle, as the lowest stimulus intensity to generate an MEP of >50μV in a peak-to-peak amplitude manner in at least 5 out of 10 trials.

A.1.3 Experimental protocol

EEG (BrainAmp MR Plus amplifiers, Brain Products) was utilized to record brain oscillations induced by TMS. Continuous brain activity was recorded by 61 electrodes situated on an elastic cap (EasyCap 64Ch, Brain Products), and the EEG signal was digitized at a sampling frequency of 5 kHz. For all electrodes, impedance was kept at <10kΩ for the entirety of the experiment. The reference electrode corresponds to FCz and is mounted on the Brain Products EEG cap

During TMS-EEG recordings, subjects were seated in a comfortable chair, and asked to stay awake with eyes open. During TMS-EEG sesssions before and after drug intake, 150 TMS pulses were administered to the FDI hotspot over the left primary motor cortex at 100% RMT intensity. In the post-drug sessions, when a change in RMT occurred, two blocks of TMS-EEG measurements at the adjusted and un-adjusted stimulation intensities were recorded. With the aim to propose the implementation of tensor decomposition on TMS-EEG data in a simple and easy-to-apply framework, we here report non-adjusted data. Random interval variation between single TMS pulses was approximately 20%, about 4s between each trial, to reduce anticipation of TMS pulse. Throughout the TMS-EEG experiment, a masking noise was applied via headphones to reduce auditory potentials evoked by TMS coil "click" sound, which would interfere with EEG recordings [4] .

A.2 Core consistency diagnostic (CORCONDIA)

The core consistency diagnostic (CORCONDIA) is a heuristic proposed by Bro and Kiers (2003) to help gauge what number of components (*n*) may be appropriate for a given PARAFAC decomposition.

CORCONDIA assesses the appropriateness of the purely multilinear PARAFAC model to represent the data. Let's recall that PARAFAC assumes the following model:

$$w_{ijk} \approx \sum_{r=1}^{n} a_{ir} \cdot b_{ir} \cdot c_{ir}. \qquad (A.1)$$

This can also be seen as:

$$w_{ijk} \approx \sum_{p=1}^{n}\sum_{q=1}^{n}\sum_{r=1}^{n} g_{pqr} \cdot a_{ip} \cdot b_{iq} \cdot c_{ir}, \qquad (A.2)$$

where

$$g_{pqr} = \begin{cases} 1 \text{ if } p = q = r, \\ 0 \text{ otherwise.} \end{cases} \qquad (A.3)$$

That is, the core tensor with elements g_{pqr} forces the interactions to be only among componentes with the same index p=q=r.

The key idea behind CORCONDIA is that, once the PARAFAC model has been computed, the component matrices **A**, **B** and **C** will used in a Tucker3 as follows:

$$w_{ijk} \approx \sum_{p=1}^{n}\sum_{q=1}^{n}\sum_{r=1}^{n} t_{pqr} \cdot a_{ip} \cdot b_{iq} \cdot c_{ir}, \qquad (A.4)$$

where the Tucker3 core tensor t_{pqr} is computed as the regression of the original data (**W**) onto the subspaces defined by the PARAFAC component matrices **A**, **B** and **C**. The Tucker3 core tensor with elements t_{pqr} would contain the perfect fit of the data onto those compoentes and it can have non-zero values at any position. In contrast, the PARAFAC model constraints its core tensor g_{pqr} to be supradiagonal [5].

Hence, the similarity between those two core tensors, the estimated t_{pqr} and the ideal g_{pqr}, can be used to measure the degree of superdiagonality of the hypothesised core tensor in PARAFAC. If the model is perfectly multilinear, the hypotethical core tensor in PARAFAC will be supradiagonal, and t_{pqr} and g_{pqr} will be identical. This will result in a CORCONDIA value of 100%. As t_{pqr} and g_{pqr} start to differ, the CORCONDIA value starts to decrease and it could eventually become negative. For a PARAFAC model with *n* components, the CORCONDIA value is computed:

$$CORCONDIA = 100\left(1 - \frac{\sum_{p=1}^{n}\sum_{q=1}^{n}\sum_{r=1}^{n}\left(g_{pqr} - t_{pqr}\right)^2}{F}\right), \qquad (\mathrm{A}.5)$$

which compares the distrivution of values in t_{pqr} and g_{pqr}, with F being the sum of the squares of the elements t_{pqr} [5].

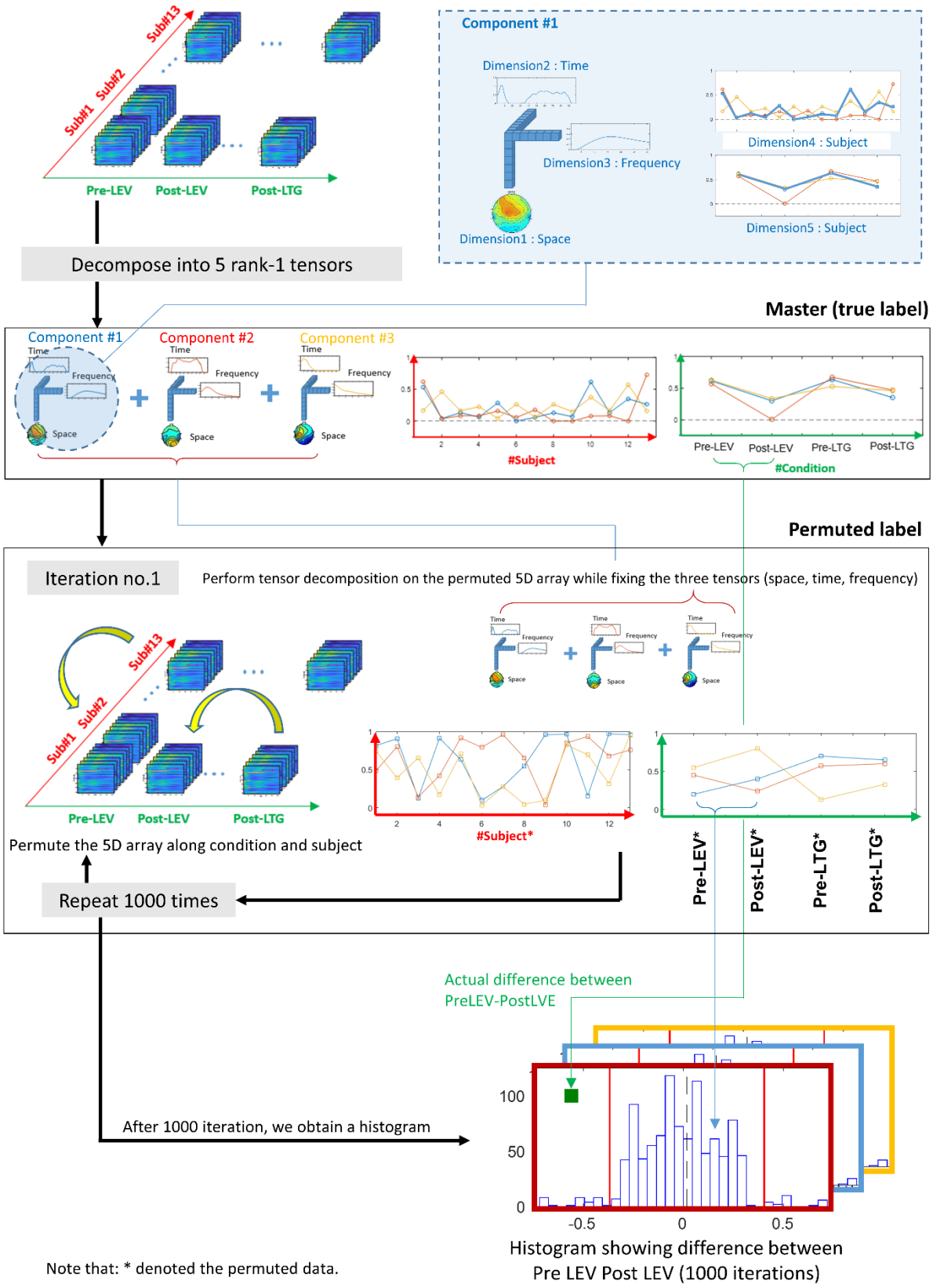

Note that: * denoted the permuted data.

Figure A1: Pipeline of statistical analysis

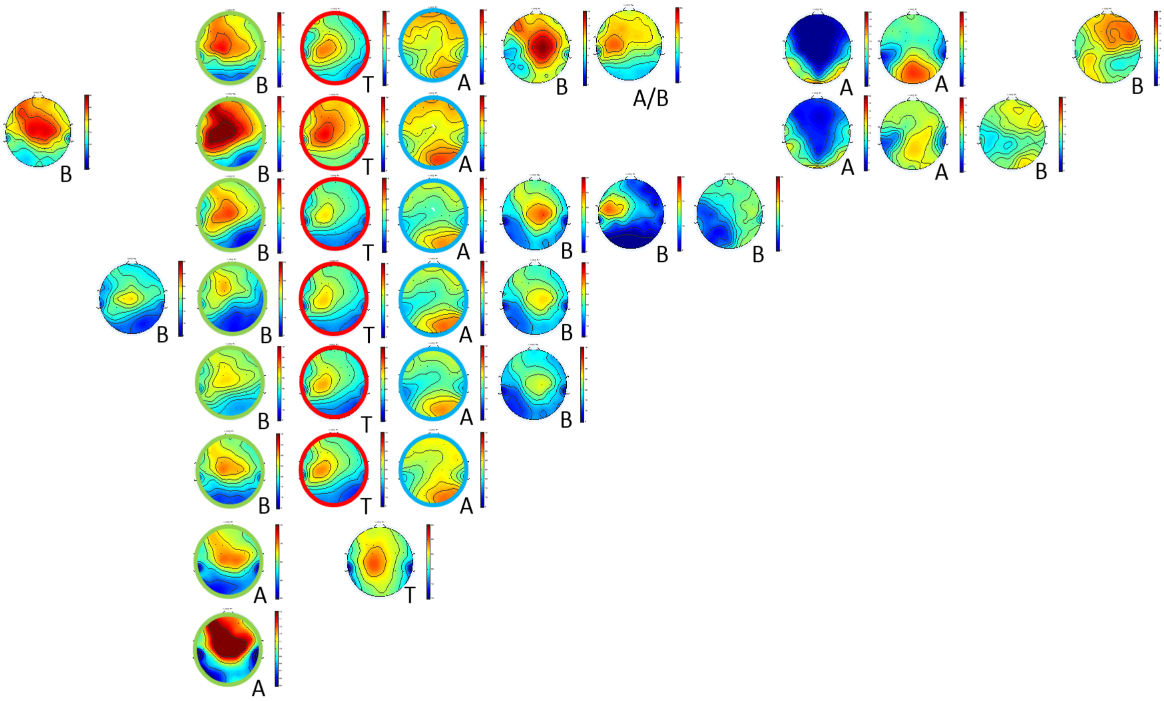

Figure A2: Each row represents topoplots of decomposed components from eight different scenarios when the number of decomposed components was varied from one to eight (bottom to top row). Here, we found three inherited spatial patterns (highlighted in green, red and blue). These patterns are found in most scenarios (at least 6 out of 8). Note that A, B, and T denote the corresponding band (A=alpha, B=Beta, and T=Theta) in the frequency domain (2^{nd} dimension).

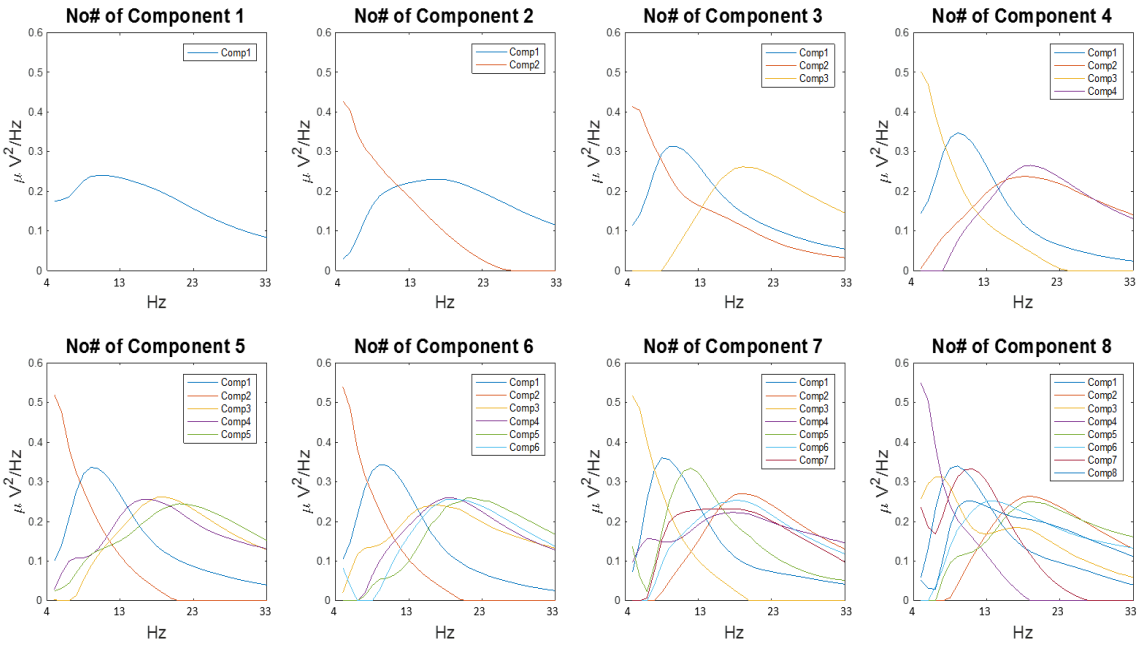

Figure A3: Each subplot shows power spectra (2nd dimension) of decomposed component(s) from eight different scenarios when a number of decomposed components was varied from one to eight.

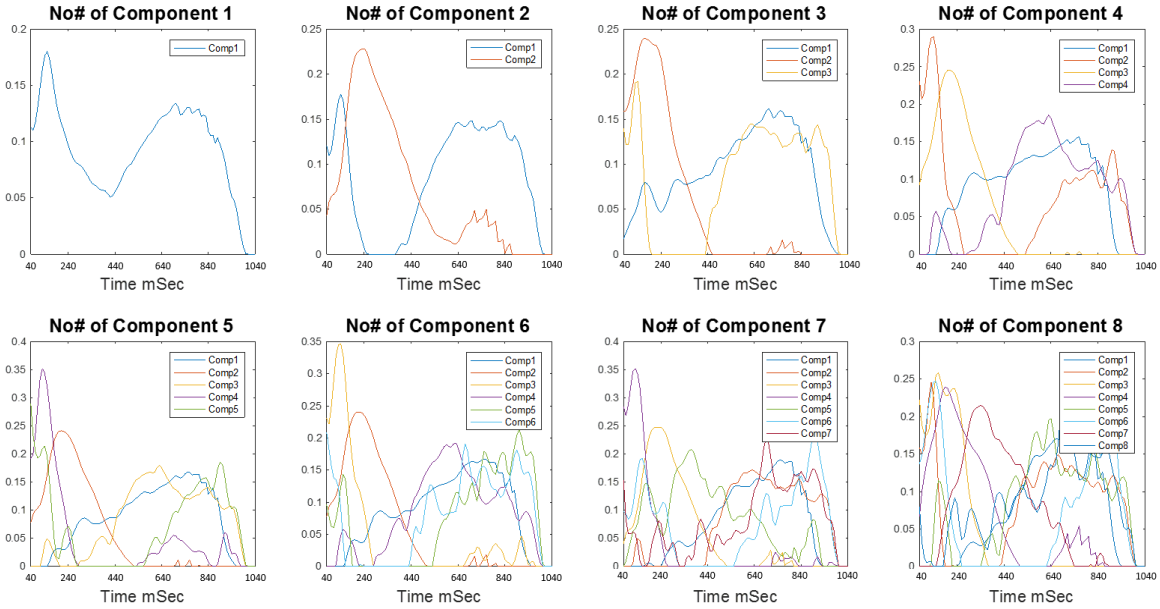

Figure A4: Each subplot shows temporal strength (3rd dimension) of decomposed components from eight different scenarios when a number of decomposed components was varied from one to eight.

Table A1: P-values from the permutation test

	Theta		Alpha		Beta	
Model2	Post LEV	Post LTG	Post LEV	Post LTG	Post LEV	Post LTG
	0.236	0.428	**0.01***	0.194	0.217	0.262
Model3	Post Placebo	Post LEV	Post Placebo	Post LEV	Post Placebo	Post LEV
	0.308	0.178	0.364	**0.015***	0.363	0.195
Model4	Post Placebo	Post LTG	Post Placebo	Post LTG	Post Placebo	Post LTG
	0.400	0.129	0.433	**0.021***	0.086	0.534

Note that: * Significant (P<0.025)

Table A2: Percentage of CORCONDIA by a number of decomposed components.

Scenario	No. of Components	CORCODIA
I	1	100.00
II	2	1.14
III	3	0.42
IV	4	-0.03
V	5	0.01
VI	6	0.00
VII	7	0.00
VIII	8	0.00

References

1 Heidegger, T., Krakow, K. & Ziemann, U. Effects of antiepileptic drugs on associative LTP-like plasticity in human motor cortex. *The European journal of neuroscience* **32**, 1215-1222, doi:10.1111/j.1460-9568.2010.07375.x (2010).

2 Cheung, H., Kamp, D. & Harris, E. An in vitro investigation of the action of lamotrigine on neuronal voltage-activated sodium channels. *Epilepsy Res* **13**, 107-112 (1992).

3 Lynch, B. A. *et al.* The synaptic vesicle protein SV2A is the binding site for the antiepileptic drug levetiracetam. *Proc Natl Acad Sci U S A* **101**, 9861-9866, doi:10.1073/pnas.0308208101 (2004).

4 Massimini, M. *et al.* Breakdown of cortical effective connectivity during sleep. *Science* **309**, 2228-2232, doi:10.1126/science.1117256 (2005).

5 Bro, R. & Kiers, H. A. L. A new efficient method for determining the number of components in PARAFAC models. *J Chemometr* **17**, 274-286, doi:10.1002/cem.801 (2003).

Reviewer comments:

Reviewer #1 (Technical Comments to the Author):

We will address the points highlighted by the reviewer in the 'Remarks to the Author section'.

1. Main figure 6 is not provided.
2. The method of TMS is not given.
3. Unclear hypothesis underlying the permutation test.
4. Figure 5. Component#2 seems dependent only on Subject #1 and #13. If so, I am not confident that the authors can infer the conclusion as the authors do about the component.
5. I often encountered typos that stop reading texts smoothly.
A couple of examples:
Discussion: In this study, we introduced a tensor decomposition method to reduce multi-dimensionality
of TMS-EEG data. We showed a ""serie"" of components which provides a parsimonious description of ""neurphysiological"" responses underlying TMS-induced oscillations. In addition we ""deminstrated"" the utility of PARAFAC...

Reviewer #1 (Remarks to the Author):

Q1. Main figure 6 is not provided, in my humble opinion.

Please accept our apology. Figure 6 was initially uploaded and successfully converted as a TIF file, but it failed to display on the pdf. In the revision, we re-uploaded the Figure.

Q2. The method of TMS is not given. We have to refer to the method in their previous paper. However, I assume that the method actually influences their results and is important. It should be more explained in this study, at least in Discussion.

As the reviewer is stating, the results relative to TMS-evoked EEG potentials modulated by lamotrigine and levetiracetam have been previously published and the specific methods are stated in Premoli et al., 2017.

With the aim not to miss details in the current work, we have specified TMS-EMG/EEG acquisition details in the supplementary materials (sections A.1.2, A.1.3) and the analysis pipeline is outlined in section 2.3.1 of the manuscript.

We are confident that the TMS methods have been described in detail.

Q3. I am not sure about the hypothesis underlying their permutation test. Please state more clearly. Why did they permute the 4th dimension (Subject), not only 5th dimension (Condition,

i.e., pre/post drug)? If they want to test the drug effect, I think the permutation of the 4th dimension is unnecessary, rather spurious, isn't it? Please explain.

The PARAFAC model employed in our work relies on a multilinear relationship between components. That is, it relies on the data having an underlying, inherent structure such that PARAFAC will estimate a one-to-one relationship between the components extracted for each dimension. The permutation test served to attest whether the extracted components had values significantly different from those that could be obtained just by random chance. Here, the random chance values could be due to 1) the drugs having no effect, and 2) the components themselves modelling uninteresting random effects in the data. In order to account for both such effects, we permuted both the 4th and 5th dimensions simultaneously. Permuting only the 5th dimension (drug) would imply that subjects with potentially higher (e.g., subject number 1 and 13) or lower power than the others would affect the permuted components in the same way as in the original data. This might be relevant if one was interested in carrying within-subject studies of the effect of the drugs which is part of future work seeking to create classifiers to predict the level of response to each drug in the subjects. However, this was not appropriate in our case as here we focused on demonstrating, for the first time, the use of tensor factorisations to model dependencies in complex data across subjects, drug condition, frequency, time and space in TMS-induced oscillations.

Q4. Figure 5. Component#2 seems dependent only on Subject #1 and #13. If so, I am not confident that the authors can infer the conclusion as the authors do about the component.

We appreciate the Reviewer's comment and agree that the small sample size affects the estimated components so that computing the PARAFAC decomposition of different subsets of subjects may lead to revealing some, but not all, of the activities founds when using the whole dataset. For example, the Reviewer is right that S1 and S13 strongly influence the presence of the alpha component. Likewise, running PARAFAC on a subset of 11 subjects without S8 and S11 means that there is a noticeable drop in the theta component. We have acknowledged this variability in the components for subsets of subjects as a limitation of the study in the "Discussion" section (on page 17, line 3-9).

Q5. Please explain more about what they cannot explain by their model (~60% variance is almost noise? Furthermore, it would be helpful for readers if the authors could add the performance of the other methodology).

We would want to emphasise that the PARAFAC model is very parsimonious. The PARAFAC model with R=3 contains a total number of elements in the estimated components smaller than 0.01% of the number of elements in the tensor. With this very small number of values, PARAFAC can account for ~40% of the explained variance in the data. The percentage of explained variance varies slightly according to the model (with an average of 41.5 and S.D. of 1.91. This suggests the stability of tensor decomposition in our data.
Furthermore, when we compare the tensor decomposition with PCA, the first three components from PCA explain 48% of the data, in comparison with the 39% explained by the three tensor components. However, it is important to consider that the total number of elements in tensor decomposition components is only 0.018% of those in the PCA components. Therefore, on average one element in the components of the tensor decomposition explains about 40,000

times more than that from PCA. This suggests tensor decomposition as a highly efficient method in representing the signature of the data.

Q6. I often encountered typos that stop reading texts smoothly.
A couple of examples:
Discussion: In this study, we introduced a tensor decomposition method to reduce multi-dimensionality
of TMS-EEG data. We showed a ""serie"" of components which provides a parsimonious description of ""neurphysiological"" responses underlying TMS-induced oscillations. In addition we ""deminstrated"" the utility of PARAFAC...

We apologise for the typos which have now been corrected throughout the manuscript.

Q7. It would corroborate their method if authors could discuss about physiological mechanism that supports their observation about the difference effect of LEV and LTG.

The proposed method does not have the aim to elucidate neurophysiological mechanism. We have discussed the current results on the light of previous investigation of LTG and LEV with TMS-EEG as follows in the discussion section 4.2:

"Results suggest that both types of drug cause similar effects on the generation of posterior alpha. The same observation derived from the investigation of these AEDs on TEPs, where despite the varying profile of effects and regardless of the (putative) molecular targets of the different drugs, systemically administered LEV and LTG exert similar modulation of TEPs (Premoli et al 2017). In addition, the effect on alpha was stronger under LEV exposure which had the highest average concentration in blood outside the reference range, with LTG averaging toward a lower concentration for its reference range (Premoli et al 2017)."

Reviewer #2 (Technical Comments to the Author):

The authors have performed this study with a good double-blind, randomized, placebo-controlled, crossover design. Even though, the authors claim the methods used are data-driven methods in my view some fine-tuning parameters like the selection of models, the number of components still do not give complete data-driven freedom to do the analyses in an automated fashion. The manuscript needs major overhauling to be able to make it understandable and to replicate the results for the readers. I point out all my major and minor comments below for each section:

Abstract:
Q1.1. The abstract does not give an overview of the current manuscript. The structure with background, methods, results and conclusions are missing.

We have re-written a well-structured abstract as follows:

'Transcranial magnetic stimulation combined with electroencephalography is a powerful tool to probe human cortical excitability. The EEG response to TMS stimulation is altered by drugs active in the brain, with characteristic "fingerprints" obtained for drugs of known mechanisms of action. However, the extraction of specific features related to drug effects is not always straightforward as the complex TMS-EEG induced response profile is multi-dimensional. Analytical approaches can rely on a-priori assumptions within each dimension or on the implementation of cluster-based permutations which do not require preselection of specific limits but may be problematic when several experimental conditions are tested.

We here propose an alternative data-driven approach based on PARAFAC tensor decomposition, which provides a parsimonious description of the main profiles underlying the multidimensional data. We validated reliability of PARAFAC on TMS-induced oscillations before extracting the features of two common anti-epileptic drugs (levetiracetam and lamotrigine) in an integrated manner.

PARAFAC revealed an effect of both drugs, significantly suppressing oscillations in the alpha range in the occipital region. Further, this effect was stronger under the intake of levetiracetam.

This study demonstrates, for the first time, that PARAFAC can easily disentangle the effects of subject, drug condition, frequency, time and space in TMS-induced oscillations.'

Methods:

We apologize for the lack of details. Given the word limit set by the journal we referred to previous publications and recognised standards within the field. Please see our replies point by point below:

Q2.1. Which reference was used for the EEG?

"The reference electrode corresponds to FCz and is mounted on the Brain Products EEG cap." This has been added to section A.1.3 in the supplementary document.

Q2.2 The reason to not to change the RMT?

We believe that ideally, in an experimental setting which involves motor cortex stimulation and in which the drug may alter RMT, two blocks of TMS-EEG measurements with adjusted and unadjusted stimulation intensity (ie. relative to RMT) should be obtained. In this specific study, we obtained data at both intensities and we have demonstrated that lamotrigine and levetiracetam have a slightly different impact on TEPs depending on whether adjusted or unadjusted stimulation intensity is used (Premoli I et al., Front Neurosci 2017). However, it is important to note that no optimal approach exists regarding the RMT adjustment and that there are advantages and disadvantages for both choices.

Adjusting stimulation intensity according to RMT ensures that corticospinal output is kept constant. However, it is unclear which specific neuronal population is responsible for the RMT changes

(corticospinal motor neurons in layer IV, connected pyramidal neurons in layer II-III, interneurons, or even spinal motor neurons) and it is unknown in which specific neuronal populations (and even in which brain regions) TEPs originate. In addition, if adjusting implies using higher stimulation intensity, this could produce by itself a stronger neuronal activation measured with EEG which may lead to misinterpretation of the results – and could have been a cause for criticism of our study. It has been shown that the amplitudes of the N45 depended on intensity in a nonlinear manner, while the amplitude of the N100 and P180 components was rather linear. Further, these changes occurred in the same cortical structures independently of stimulus intensities (Komssi et al., 2004). Therefore, not adjusting guarantees constant electric fields in the motor cortex to stimulate the motor neurons. Thus, re-adjustment of RMT could be either helpful or an additional potential confound when investigating changes in TMS-evoked/induced oscillatory activity after drug intake (or any other intervention).

With the aim to propose the implementation of tensor decomposition on TMS-EEG data in a simple and easy-to-apply framework, we have decided to use the non-adjusted data here.

See changes in supplementary material section A.1.3

"In the post-drug sessions, when a change in RMT occurred, two blocks of TMS-EEG measurements at the adjusted and un-adjusted stimulation intensities were recorded. With the aim to propose the implementation of tensor decomposition on TMS-EEG data in a simple and easy-to-apply framework, we here report non-adjusted data."

Q2.3 What type of filters were used for the artifact correction is not mentioned which could affect the output of the ICA?

We have now provided more detail in section 2.3.1 of the manuscript as follows:

"After excluding records/trials with prominent eye movements, blinks, and muscle artefacts (on the basis of visual inspection), EEG data was analyzed using an established multistep procedure (Premoli et al. 2017). Data was down sampled to 1 kHz, segmented 1 s before and after the pulse, and linearly interpolated for ±10 ms to remove the TMS artefact. Bad channels were removed from the EEG, and the signal was reconstructed by interpolating the surrounding electrode signals. Data was then notched filtered (50 Hz). Independent Component analysis (ICA) was applied to remove TMS-related artifacts (i.e., the cranial muscle response, the recharging of capacitors, and related exponential decay artifacts (Herring et al., 2015; Korhonen et al., 2011; Rogasch et al., 2014), as well as further muscle and ocular activity. Finally, remaining data were re-referenced to the average of all electrodes, baseline corrected (from -1000 to -50 ms) and band-pass filtered (1-80 Hz)."

Q2.4 Not clear from the text whether baseline correction was done? Also, the baseline type was absolute or relative?

We have now provided more detail in section 2.3.1 of the manuscript as follows:

"After that, for each segment we estimated its time-frequency plot by applying a Hanning taper windowed fast Fourier transform (FFT) with frequency-dependent window length (width: 3.5 cycles per time window, time steps: 10 ms, frequency steps: 1 Hz from 4 to 45 Hz) [35]. TMS-induced responses were obtained by subtracting the individual time-domain average from each trial before calculating the TF of the single trials (as done in Cohen and Donner, 2013). We performed single-trial normalization by z-transforming the TF of each trial for each frequency. The z-transformation was based on the respective mean and standard deviation derived from the full trial length. This was followed by an absolute baseline correction for each trial, by subtracting the average of the 1000 to 50 ms period for each frequency to ensure z-values represented a change from pre-TMS baseline."

Q2.5. After the FFT the authors explain that they end up with an array of 61×42×201 by taking into consideration (4 to 45 Hz). I understand due to the TMS artifact to select 40 ms after the TMS effect but why did the authors reduce the frequency to 32 Hz is not clear to me?

We decided to trim the original array of 61x42x201 into 61x31x98 for two reasons:

1) *As mentioned by the reviewer, to avoid the TMS artefacts we select the data starting from 40 milliseconds. This reduced the 3rd dimension from 201 to 98.*
2) *We decided not to include any frequency bin above 34 Hz to minimise contamination from muscle activities and to be comparable with our previous paper which focused on the on alpha and beta bands. Therefore, the 2nd dimension reduced from 42 to 31.*

Q2.6. Which variables were included in Model 1?

To our knowledge, Tensor decomposition has never been implemented in TMS-EEG before. We used model-1 as a proof-of-concept to study the decomposed component from the condition without any effect from drug and visually inspected for their physiological meaning

(as explained on page 9 lines 9-11).

Q2.7. In section 2.3.4 the non-negativity factorization of the matrix is not clear to me why this was applied?

Non-negativity simplifies the interpretation of the results substantially since any components found under this constraint can only interact constructively, not destructively. That is, they cannot cancel each other out (either fully or partially). We decided to impose this constraint for two reasons:

1) *the positive elements account for a majority of the data (~56%, whereas the negative elements are about 32%, and 12% zero), and the mean average of the positive elements is about 1.7 times as compared to that of the negative element,*
2) *for ease of interpretation.*

Note that the choice to impose this constraint was decided before we started analysing the data.

Q2.8. I think this is a major shortcoming in the manuscript to choose the components based on two criteria namely 1) the explained variance and 2) CORCONDIA. I would have preferred to use the variance which is a good measure and the robustness of identifying the components by a cluster analyses instead of manual visualization of the components.

We are thankful for this suggestion and agree that the decision on the number of components was mostly based on the percentage of explained variance. Hence, we have revised the manuscript to focus on that criterion, together with the interpretability of the extracted components. We still report the CORCONDIA values for completeness, but they have been moved to supplementary material.

Furthermore, we performed k-mean clustering in the 1st, 2nd, and 3rd components (space, frequency, time, respectively) shown in the supplementary figures A2-A4 and found that according to the elbow method (see Figure B1), three is the optimal number of clusters. This strengthens our choice in choosing three as the optimal number of decomposed components.

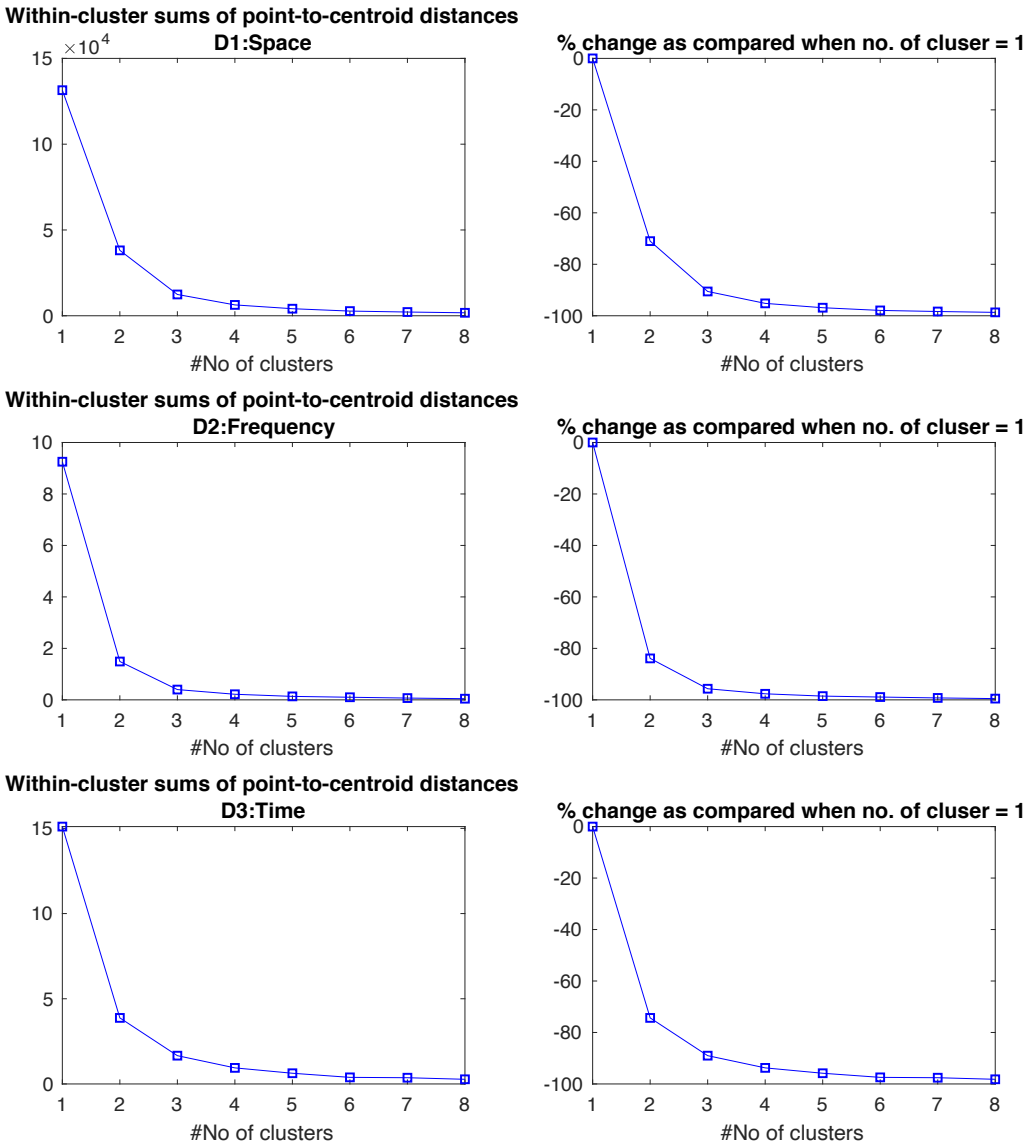

Figure B1: The left panel shows the change of sums of point-to-centroid distances with each cluster (from D1 (top) to D3 (bottom). The right panel shows the change in %.

Results:

Q3.1. The number of components was selected based on the two parameters which are listed in Table 1. As shown the explained variance of 29.14% for the first component whereas the CORCONDIA gives 100.00 for later detected components this constraint barely as any contribution why are their contradicting results?

CORCONDIA and the percentage of explained variance are opposing criteria in the sense that CORCONDIA will decrease with the number of components, whereas the percentage of explained variance will increase. For clarity and conciseness, we have move CORCONDIA to the supplementary

material and focused on the percentage of explained variance. Furthermore, the contradiction between explained variance at 29.14% and CORCONDIA of 100 emphasized the fact our 5D tensor is not fully multilinear form, in which the number of optimal components is different across dimension. We decided using PARAFAC to reserve one-to-one relations along component for ease of interpretation as described in section 4.1.

Q3.2. The end selection of the components authors state the explained variance was 40%? How was the consistency across 1000 permuted iterations for the 4th and 5th dimension?

We found the explained variance very consistent with the average of 39.30 with SD of 0.08.

Q3.3. What is the reason to choose the theta (4-6 Hz), alpha (6-13 Hz) and Beta (15-30 Hz) frequency bands instead of the normal nomenclature of 4-7, 8-13, 14-30 Hz? Did the 6 Hz data was used in both the frequency bands will have influence in the PARAFAC results?

We chose to denote the components with peak frequency between 4-6Hz, 6-13Hz, and 15-30Hz as 'theta', 'alpha', and 'beta', respectively. As these frequency ranges appeared in our Figures, we did not intend to redefine the traditional nomenclature of EEG. In fact, each component is a weighted sum of all frequency between 4 to 34 Hz. For example, in model 2 (LEV vs LTG), the alpha band reach its peak between 6-13Hz, but the component itself is a weighted sum of all frequency starting 4 to 34 Hz. To avoid any confusion, we amended the caption underneath Figure 3.

Q3.4. Figure 4 legend is not clear "three components during pre-drug and post-drug" The D should be mentioned in the figure legend represent the dimensions. Similarly also to refer to the figure when it is discussed in the results section (for. ex: Intersubject variabilities in section 3.3).

This has been corrected see line 22 on page 17.

Discussion:

Q4.1. In the discussion, there is brief mention about multilinear form for the CONCORDIA results, however, no further interpretation what does this mean physiologically?

Javier

Physiologically, an entirely multilinear, one-to-one, relationship between components would mean that a topographical map of activity over the scalp is characterised by only one frequency response and temporal evolution, and that such combination of profiles can be unambiguously related to a pattern of drug response to which the subjects would be more or less sensitive according to their levels in the components for the subject domain.

Q4.2. For the claim in discussion section 4.2 that the three components are highly similar needs cluster statistics on the identified components.

We checked the similarity between each component across four models using cosine distance [0 = no difference]. The mean difference across all component, frequency, and model is 0.073 with SD = 0.05. In conclusion, we found the spatial components with highest similar across all models, following by the frequency components and the time components, respectively.

Table B1: Mean and standard deviation of cosine distance values across four models.

Frequency Band	Dimension 1	Dimension 2	Dimension 3
	Space	Frequency	Time
Theta	0.0085 (SD=0.0067)	0.0152 (SD=0.0152)	0.0318 (SD=0.0393)
Alpha	0.0404 (SD=0.0308)	0.1208 (SD=0.1480)	0.2011 (SD=0.2108)
Beta	0.0230 (SD=0.0127)	0.1056 (SD=0.1435)	0.1082 (SD=0.1223)

SD = standard deviation

Q4.3. The change only found in the alpha range could be due to the non-negativity constraint applied. Did the authors check the results with the non-negativity constraint?

As answered in question Q.2.7, we chose to impose the non-negativity constraint for ease of interpretation, and more than half of the elements are positive, and only a third of the elements are negative (with the average amplitude about the half of the positive elements). Nevertheless, we acknowledge that the non-negativity constraint might have had an effect on the results by preventing us from finding negative patterns. Figure B2 shows the difference between the decomposed components with and without non-negativity constraint. Unlike the non-negativity case, the occipital alpha was not extracted when the constraint was not applied. As a consequence, no significant difference was found. The alpha component, in this case, was spatially overlapped with the beta component. We have acknowledged this potential limitation in the Discussion (on page 17, lines 3-9).

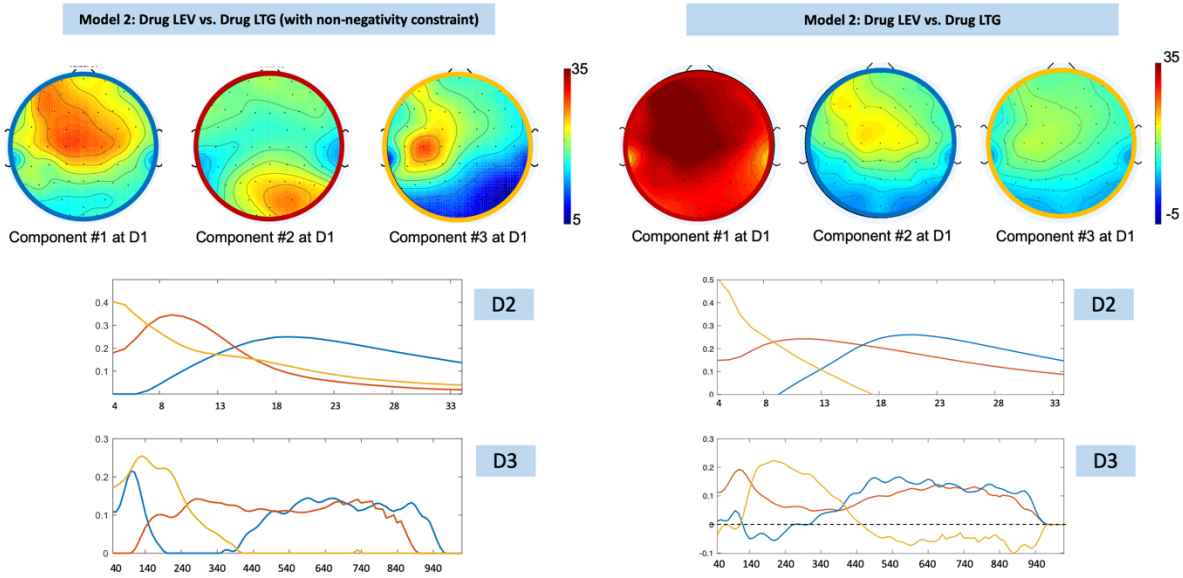

Figure B2: (Left) Decomposed components on 1st, 2nd, and 3rd dimensions when the non-negativity constraint was applied (as shown in the manuscript). (Right) Decomposed components on 1st, 2nd, and 3rd dimensions without constraint.

Minor comments:

All typos have been now corrected.

- **i.e. some parts the acronym is written as ie.**
- **AED acronym first usage is not defined before in the manuscript**
- **Section 2.3.3 comonents should be components**

- It would be helpful to explain the acronyms used in the figures also in the figure legend

- graps should be grasp in the disucssion section 4.1
- **Adknowledgements change to Acknowledgements**
- **JE acknoledges change to acknowledges**
- **IP collteced and preprocesed change to collected and preprocessed**
- **Contirbutions: All authors reviewed the manuscript**
- **declar change to declare in COI**